

Los Alamos

NATIONAL LABORATORY

memorandum

Los Alamos Neutron Science Center, LANSCE-1
Accelerator Physics and Engineering Group

To: Distribution
From: Barbara Blind, LANSCE-1, H808
Robert Garnett, LANSCE-1, H817
Phone/Fax: 5-2607/5-2904
Symbol: LANSCE-1:99-063
Date: April 8, 1999
Email: bblind@lanl.gov

SUBJECT: Discussion of 14-Quadrupole SNS MEBT

Introduction

John Staples of LBNL has introduced a 14-quadrupole SNS MEBT. Just like the 18-quadrupole baseline MEBT described in an earlier memo [1], this MEBT has three distinctive sections. The first section has four quadrupoles (Q1 through Q4) and one buncher cavity (B1), the second section (center section) has six quadrupoles (Q5 through Q10) and two buncher cavities (B2 and B3) and houses the chopper and antichopper, and the third section has four quadrupoles (Q11 through Q14) and one buncher cavity (B4). Figure 1 shows a layout of the 14-quadrupole MEBT, generated by TRACE 3-D. The beam envelope shown in Figure 1 ends at the entrance to the DTL.

This memo discusses the performance of the 14-quadrupole MEBT, with two different foci. They are referred to as the initial match and the improved match. The performance of the two foci is similar. Also, the performance is comparable to that of the modified baseline MEBT [1]. However, the separation between the undeflected and the fully deflected beam at the approximate chopper-stopper location is better for the 14-quadrupole MEBTs than for the modified baseline MEBT.

Performance of 14-Quadrupole MEBT With Initial Match

The center section of the 14-quadrupole MEBT has elements that are arranged in a mirror-image configuration. The quadrupoles of the center section were operating as quadrupole pairs (Q5 and Q10, Q6 and Q9, Q7 and Q8) but the cavities originally had different settings. Thus, this configuration would not have restored the deflected beam back to the axis downstream of the antichopper.

We adjusted B3 to the same setting as B2, and then adjusted Q6 and Q9 (as a pair) so that the deflected beam is restored back to the axis.

The properties of this MEBT were then studied with TRACE 3-D. As an input beam, a beam with the parameters of the output beam of the RFQ without errors was used. At the midpoint of the center section, this beam had Twiss parameters of $\alpha_x = -0.416$, $\beta_x = 4.608$ m, $\alpha_y = -0.204$, $\beta_y = 0.956$ m. We adjusted Q1 through Q4 to achieve a beam with $\alpha_x = 0.0$, $\beta_x = 4.6$ m, $\alpha_y = 0.0$, $\beta_y = 0.956$ m at the midpoint of the center section.

For the 14-quadrupole MEBT, the midpoint of the center section is the approximate chopper-stopper location. The fully deflected beam (the beam that is deflected by the chopper by 20 mrad) is off axis at that location by 1.109 cm. For the baseline MEBT, the fully deflected beam was off axis at the approximate chopper-stopper location by only 0.835 cm.

The 9269-macroparticle RFQ output beam discussed in the earlier memo was tracked through the 14-quadrupole MEBT without errors to the approximate chopper-stopper location. Figure 2 shows the footprints of the undeflected and fully deflected beam at that location. An aperture that removes all of the fully deflected beam should not interfere in a substantial way with the undeflected beam. The separation between fully deflected and undeflected beam at the approximate chopper-stopper location is better than for the modified baseline MEBT.

Quadrupoles Q11 through Q14 and buncher cavity B4 were used to match the beam to the DTL. The transverse match was perfect, due to the use of four quadrupoles. The longitudinal match was only approximately correct, due to the use of only one buncher cavity. There was a 20% mismatch, longitudinally.

Appendix A shows the settings of the quadrupoles and buncher cavities for the 14-quadrupole MEBT with the initial match.

Earlier, we had studied the performance of the baseline MEBT and the modified baseline MEBT. Each study had consisted of the tracking of ten RFQ output beams through ten machines with different sets of errors. The study of the performance of the 14-quadrupole MEBT was done in the same way. However, there were two basic differences. The 14-quadrupole MEBT was designed by John Staples assuming an RFQ output beam (MEBT input beam) with horizontal and vertical Twiss parameters that are reversed from those assumed for the baseline MEBT. This is equivalent to rolling the RFQ by 90°. Thus, the coordinates of the ten RFQ output beams had to be transformed accordingly, before use as input beams for the 14-quadrupole MEBT. This involved setting $x_{\text{new}}=y_{\text{old}}$, $x'_{\text{new}}=y'_{\text{old}}$, $y_{\text{new}}=-x_{\text{old}}$ and $y'_{\text{new}}=-x'_{\text{old}}$. Also, the baseline MEBT had 18 quadrupoles that were being assigned errors, versus 14 quadrupoles for the MEBT discussed here. However, the same sets of random numbers were being used to describe the MEBT errors. Thus, for instance, the misalignment of the first quadrupole of the center section of the 14-quadrupole MEBT was equal to the misalignment of the fifth quadrupole of the first section of the baseline MEBT, with the same correspondence between the fractional gradient errors. The errors in the DTL, the CCDTL and the CCL were identical to those of the earlier studies. The error limits for the transverse misalignments of the MEBT quadrupoles were set to 5 mil. The rectangular apertures were opened up, as shown in Appendix A, to avoid beam losses.

The transverse and longitudinal rms emittances in the MEBT are shown in Figure 3, top, and the maximum beam extents are shown in Figure 3, bottom. Figure 4, top and bottom, shows the same for the DTL, and Figure 5, top and bottom, shows the same for the

CCDTL and CCL. Figures 3, 4, and 5 are to be compared to Figures 9, 10, and 11 of the earlier memo.

For the 14-quadrupole MEBT with the initial match, the transverse rms emittances at the exit of the CCL are between 0.0270π -cm-mrad and 0.0313π -cm-mrad and the longitudinal rms emittances are between 0.0471π -cm-mrad and 0.0643π -cm-mrad. For the modified baseline MEBT, the transverse rms emittances had ranged between 0.0272π -cm-mrad and 0.0312π -cm-mrad, and the longitudinal rms emittances had ranged between 0.0497π -cm-mrad and 0.0616π -cm-mrad. Thus, the values cover larger ranges for the 14-quadrupole MEBT, but the averages are about the same for this MEBT and the modified baseline MEBT. Through the MEBT, the transverse rms emittances and especially the longitudinal rms emittances stay at lower values for the 14-quadrupole MEBT than for the modified baseline MEBT.

Beam losses were later assessed by tracking the beams through the MEBT with the apertures representing the chopper and antichopper plates inserted. The only particle losses occurred at the downstream end of the antichopper. The losses were 12 macroparticles for run 4, 9 for run 6, 143 for run 9, and 72 for run 10. The effect of partial steering was simulated by reducing the error limits for the transverse misalignments of the MEBT quadrupoles from 5 mil to 2 mil. Now, 1 macroparticle was lost in run 6, 4 in run 9 and 3 in run 10. Without any transverse misalignments, there are no particle losses. This means that good alignment or some steering is required to avoid particle losses.

Performance of 14-Quadrupole MEBT With Improved Match

The MEBT can be tuned for a proper transverse and longitudinal match using quadrupoles Q11 through Q14 and buncher cavities B3 and B4. However, when B3 is adjusted, quadrupoles Q6 and Q9 must be adjusted for the proper phase advance through the center section. Moreover, Q6 and Q9 must be adjusted individually, as opposed to as a pair, since the mirror symmetry in the settings of the center-section elements is broken. Then, the beam envelope through the center section is no longer symmetric around the midpoint of the center section.

Instead, in a first iteration we adjusted B2 and B3 as a pair, and Q11 through Q14 to match the beam to the DTL. In a second iteration, we then adjusted first Q6 and Q9 (as a pair) for the proper phase advance through the center section and then B4 and Q11 through Q14. The transverse match is again perfect and the longitudinal match is improved from 20% mismatch to 5% mismatch.

Appendix B shows the settings of the quadrupoles and buncher cavities for the 14-quadrupole MEBT with the improved match. Figure 6 shows the beam-profile plots in the MEBT and DTL. Figure 7 shows the beam phase-space plots at the end of the MEBT (top) and at the end of the DTL (bottom).

We repeated the performance study for the 14-quadrupole MEBT with the improved match. The transverse and longitudinal rms emittances in the MEBT are shown in Figure 8, top, and the maximum beam extents are shown in Figure 8, bottom. Figure 9, top and bottom, shows the same for the DTL, and Figure 10, top and bottom, shows the same for the CCDTL and CCL. The transverse rms emittances at the exit of the CCL are between 0.0268π -cm-mrad and 0.0309π -cm-mrad and the longitudinal rms emittances are between 0.0455π -cm-mrad and 0.0621π -cm-mrad. The longitudinal rms emittances at the exit of the MEBT are larger for the 14-quadrupole MEBT with the improved match than for the 14-quadrupole MEBT with the initial match. The values have about the same upper limit as for the baseline MEBT, but there is a larger range of values. The same is true at the exit of the CCL.

Summary

The 14-quadrupole MEBT that was matched with a single buncher cavity and four quadrupoles (initial match) and the 14-quadrupole MEBT that was matched in the iterative process described above (improved match) have similar performance, even though the longitudinal mismatch of the DTL input beam was reduced from 20% to 5%. This result is consistent with the mismatch sensitivity study done earlier [2], which showed little or no effect on transverse or longitudinal rms output-beam emittance for mismatches up to about 20%. The performance of the 14-quadrupole MEBTs is also comparable to the performance of the modified baseline MEBT.

Careful steering through the center sections of the 14-quadrupole MEBTs is essential to avoid beam losses at the plates of the antichopper.

For the matching to the DTL, the output beam from an RFQ without errors was used, with a MEBT without errors. It remains to be seen whether the emittance growth can be reduced when a more realistic MEBT input beam is used for matching to the DTL.

References

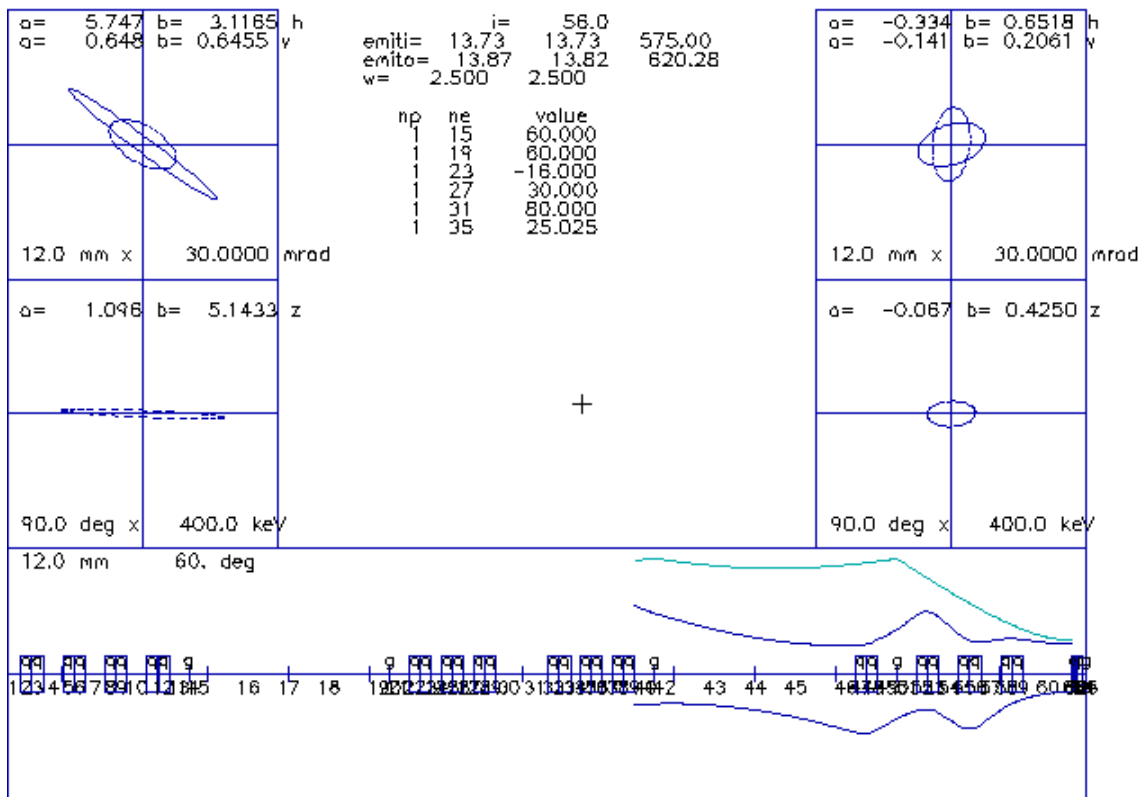
- [1] Barbara Blind and Robert Garnett, "SNS Baseline MEBT and Modified Baseline MEBT", LANSCE-1:99-061, April 5, 1999.
- [2] R. W. Garnett, "SNS 1-Tank DTL Input Beam Missteering and Mismatch Sensitivity Study", LANSCE-1:99-053, March 23, 1999.

Appendix A. Excerpt from PARMILA input deck
for 14-quadrupole MEBT with initial match.

```
trans1 1 1 0.0e-1 1 2.0 0 1 1
trans1 2 1 4.0 2 2.0 0 1 1
trans1 3 3 -3052.950 7.0 2.0 1 1 1
trans1 4 1 6.0 2 2.0 0 1 1
trans1 5 3 3112.944 7.0 2.0 1 1 1
trans1 6 1 6.0 2 2.0 0 1 1
trans1 7 3 -3267.645 7.0 2.0 1 1 1
trans1 8 1 6.0 2 2.0 0 1 1
trans1 9 3 2370.605 7.0 2.0 1 1 1
trans1 10 1 6.0 3 2.0 0 1 1
trans1 11 2 0.075 -90. 1 2.0 0 0
trans1 12 1 6.0 4 2.0 0 1 1
trans1 13 7 2.0 2.0
trans1 14 1 25.0 10 2.0 0 1 1
trans1 15 7 2.0 2.0
trans1 16 20 0.0 0.0 0.0 0.0
trans1 17 1 25.0 10 2.0 0 1 1
trans1 18 7 2.0 2.0
trans1 19 1 6.0 2 2.0 0 1 1
trans1 20 2 0.040 -90. 1 2.0 0 0
trans1 21 1 6.0 2 2.0 0 1 1
trans1 22 3 -1600.0 7.0 2.0 1 1 1
trans1 23 1 3.0 2 2.0 0 1 1
trans1 24 3 2502.480 7.0 2.0 1 1 1
trans1 25 1 3.0 2 2.0 0 1 1
trans1 26 3 -1100.0 7.0 2.0 1 1 1
trans1 27 1 8.0 4 2.0 0 1 1
trans1 28 7 2.0 2.0
trans1 29 1 8.0 4 2.0 0 1 1
trans1 30 3 -1100.0 7.0 2.0 1 1 1
trans1 31 1 3.0 2 2.0 0 1 1
trans1 32 3 2502.480 7.0 2.0 1 1 1
trans1 33 1 3.0 2 2.0 0 1 1
trans1 34 3 -1600.0 7.0 2.0 1 1 1
trans1 35 1 6.0 2 2.0 0 1 1
trans1 36 2 0.040 -90. 1 2.0 0 0
trans1 37 1 6.0 2 2.0 0 1 1
trans1 38 7 2.0 2.0
trans1 39 1 25.0 10 2.0 0 1 1
trans1 40 7 2.0 2.0
trans1 41 20 0.0 0.0 0.0 0.0
trans1 42 1 25.0 10 2.0 0 1 1
trans1 43 7 2.0 2.0
trans1 44 1 6.0 2 2.0 0 1 1
trans1 45 3 1660.5376 7.0 2.0 1 1 1
trans1 46 1 6.0 3 2.0 0 1 1
trans1 47 2 0.1041 -90. 1 2.0 0 0
trans1 48 1 6.0 3 2.0 0 1 1
trans1 49 3 -2812.9142 7.0 2.0 1 1 1
trans1 50 1 6.0 3 2.0 0 1 1
trans1 51 3 2661.0065 7.0 2.0 1 1 1
trans1 52 1 6.0 3 2.0 0 1 1
trans1 53 3 -863.1402 7.0 2.0 1 1 1
trans1 54 1 15.0 3 2.0 0 1 1
trans1 55 19 0 0
trans1 56 3 -6700.0 1.75 1.25 0 1 1
```

Appendix B. Excerpt from PARMILA input deck
for 14-quadrupole MEBT with improved match.

```
trans1 1 1 0.0e-1 1 2.0 0 1 1
trans1 2 1 4.0 2 2.0 0 1 1
trans1 3 3 -3052.950 7.0 2.0 1 1 1
trans1 4 1 6.0 2 2.0 0 1 1
trans1 5 3 3112.944 7.0 2.0 1 1 1
trans1 6 1 6.0 2 2.0 0 1 1
trans1 7 3 -3267.645 7.0 2.0 1 1 1
trans1 8 1 6.0 2 2.0 0 1 1
trans1 9 3 2370.605 7.0 2.0 1 1 1
trans1 10 1 6.0 3 2.0 0 1 1
trans1 11 2 0.075 -90. 1 2.0 0 0
trans1 12 1 6.0 4 2.0 0 1 1
trans1 13 7 2.0 2.0
trans1 14 1 25.0 10 2.0 0 1 1
trans1 15 7 2.0 2.0
trans1 16 20 0.0 0.0 0.0 0.0
trans1 17 1 25.0 10 2.0 0 1 1
trans1 18 7 2.0 2.0
trans1 19 1 6.0 2 2.0 0 1 1
trans1 20 2 0.0360788 -90. 1 2.0 0 0
trans1 21 1 6.0 2 2.0 0 1 1
trans1 22 3 -1600.0 7.0 2.0 1 1 1
trans1 23 1 3.0 2 2.0 0 1 1
trans1 24 3 2499.441 7.0 2.0 1 1 1
trans1 25 1 3.0 2 2.0 0 1 1
trans1 26 3 -1100.0 7.0 2.0 1 1 1
trans1 27 1 8.0 4 2.0 0 1 1
trans1 28 7 2.0 2.0
trans1 29 1 8.0 4 2.0 0 1 1
trans1 30 3 -1100.0 7.0 2.0 1 1 1
trans1 31 1 3.0 2 2.0 0 1 1
trans1 32 3 2499.441 7.0 2.0 1 1 1
trans1 33 1 3.0 2 2.0 0 1 1
trans1 34 3 -1600.0 7.0 2.0 1 1 1
trans1 35 1 6.0 2 2.0 0 1 1
trans1 36 2 0.0360788 -90. 1 2.0 0 0
trans1 37 1 6.0 2 2.0 0 1 1
trans1 38 7 2.0 2.0
trans1 39 1 25.0 10 2.0 0 1 1
trans1 40 7 2.0 2.0
trans1 41 20 0.0 0.0 0.0 0.0
trans1 42 1 25.0 10 2.0 0 1 1
trans1 43 7 2.0 2.0
trans1 44 1 6.0 2 2.0 0 1 1
trans1 45 3 1607.1074 7.0 2.0 1 1 1
trans1 46 1 6.0 3 2.0 0 1 1
trans1 47 2 0.105263 -90. 1 2.0 0 0
trans1 48 1 6.0 3 2.0 0 1 1
trans1 49 3 -2797.4694 7.0 2.0 1 1 1
trans1 50 1 6.0 3 2.0 0 1 1
trans1 51 3 2781.8543 7.0 2.0 1 1 1
trans1 52 1 6.0 3 2.0 0 1 1
trans1 53 3 -1147.3006 7.0 2.0 1 1 1
trans1 54 1 15.0 3 2.0 0 1 1
trans1 55 19 0 0
trans1 56 3 -6700.0 1.75 1.25 0 1 1
```



09:32:12.33 04/07/99

Figure 1. Layout of SNS 14-quadrupole MEFT.

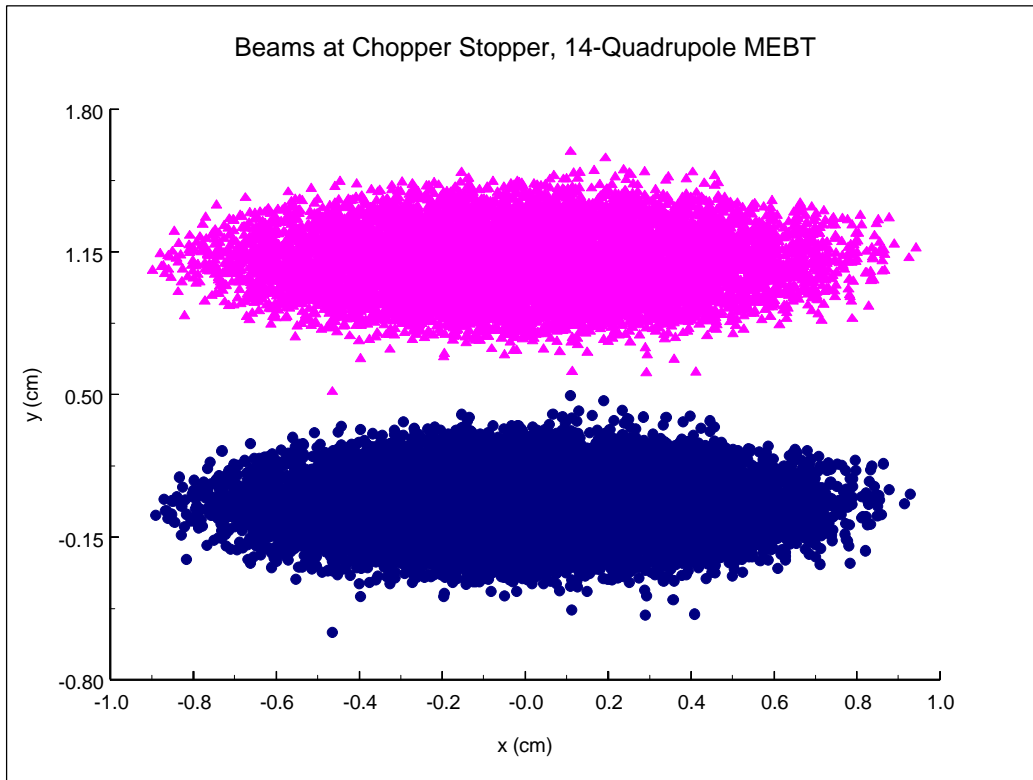


Figure 2. Footprints of undeflected and fully deflected beam at chopper stopper.

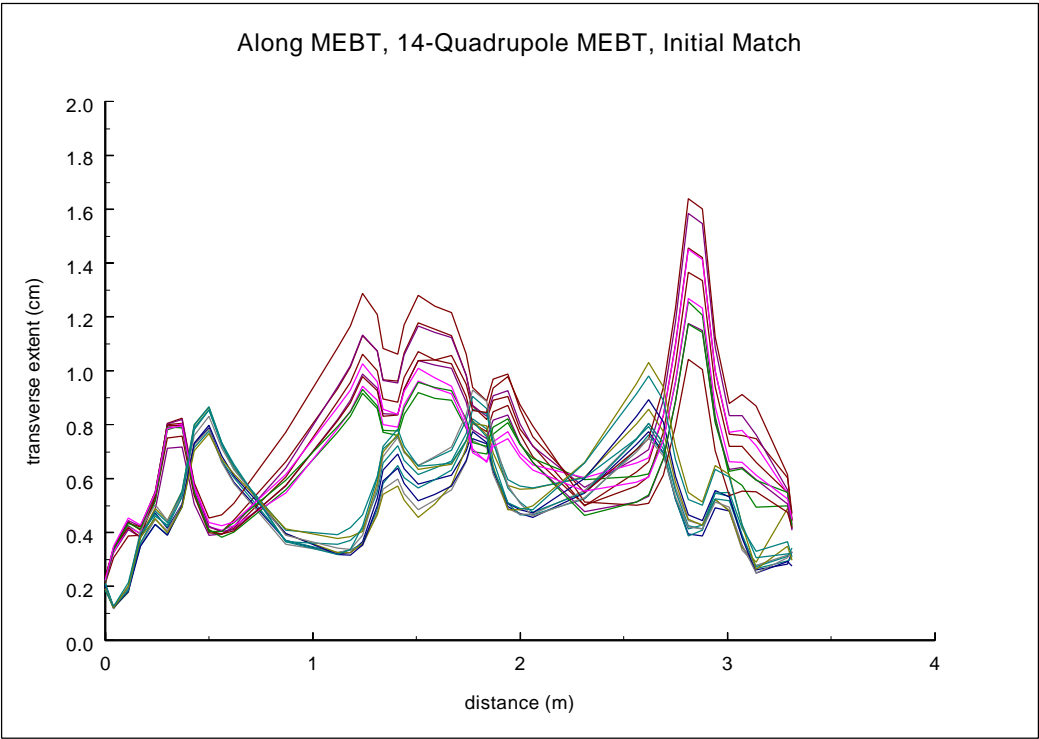
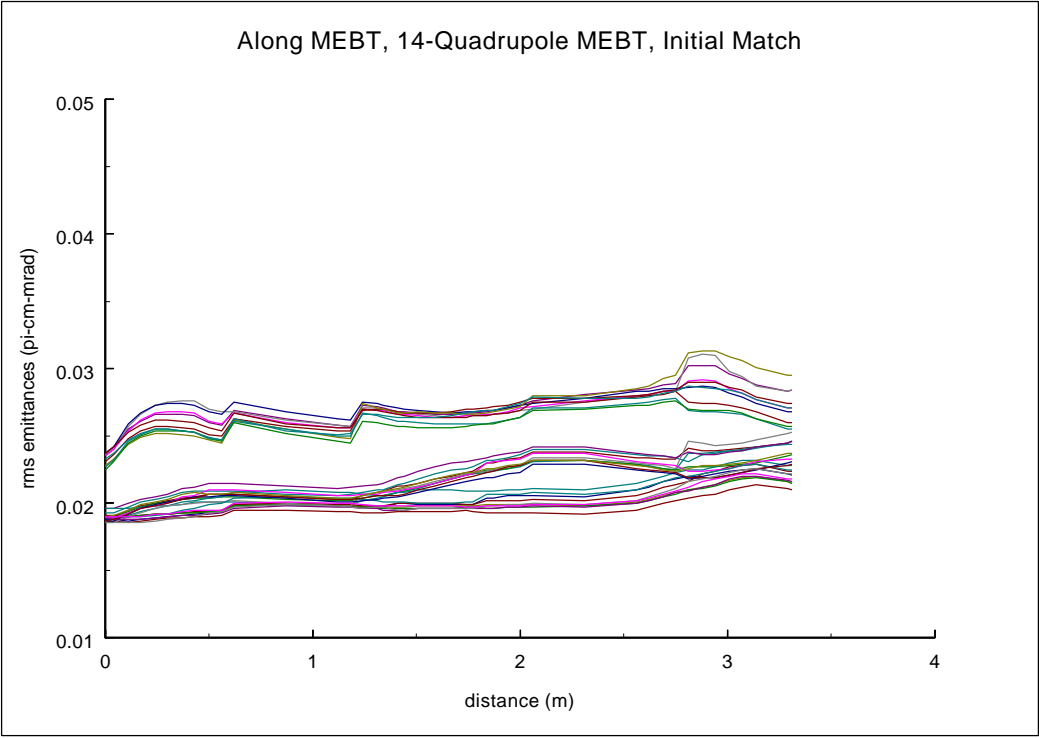


Figure 3. Transverse and longitudinal rms emittances (top) and maximum beam extents (bottom) in MEBT, for initial match.

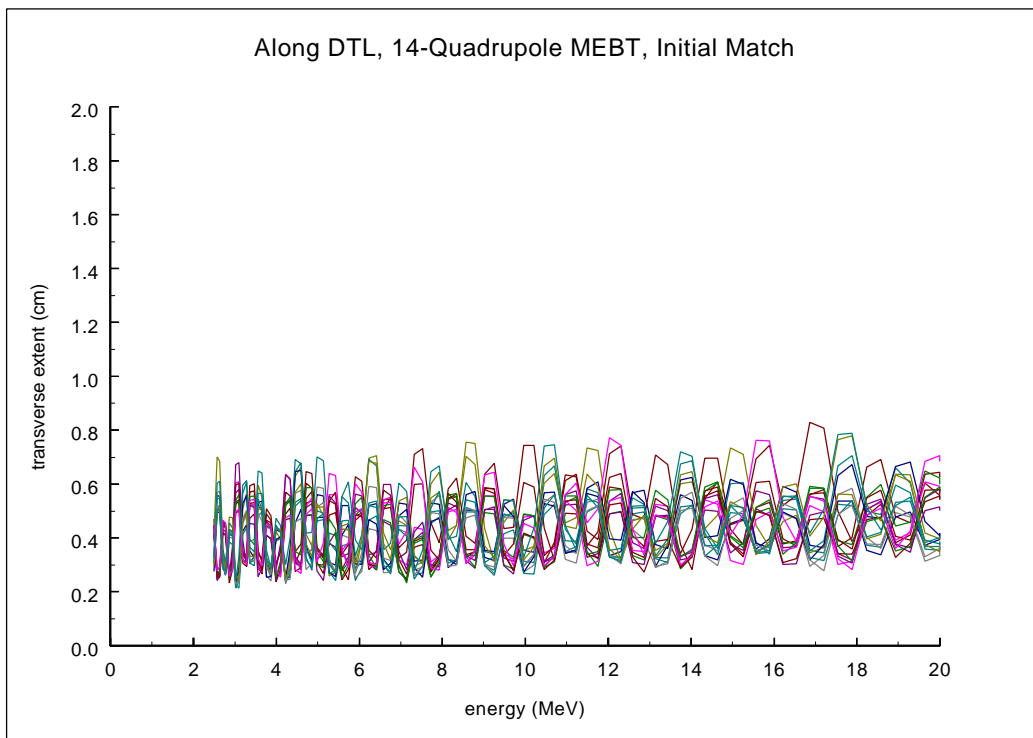
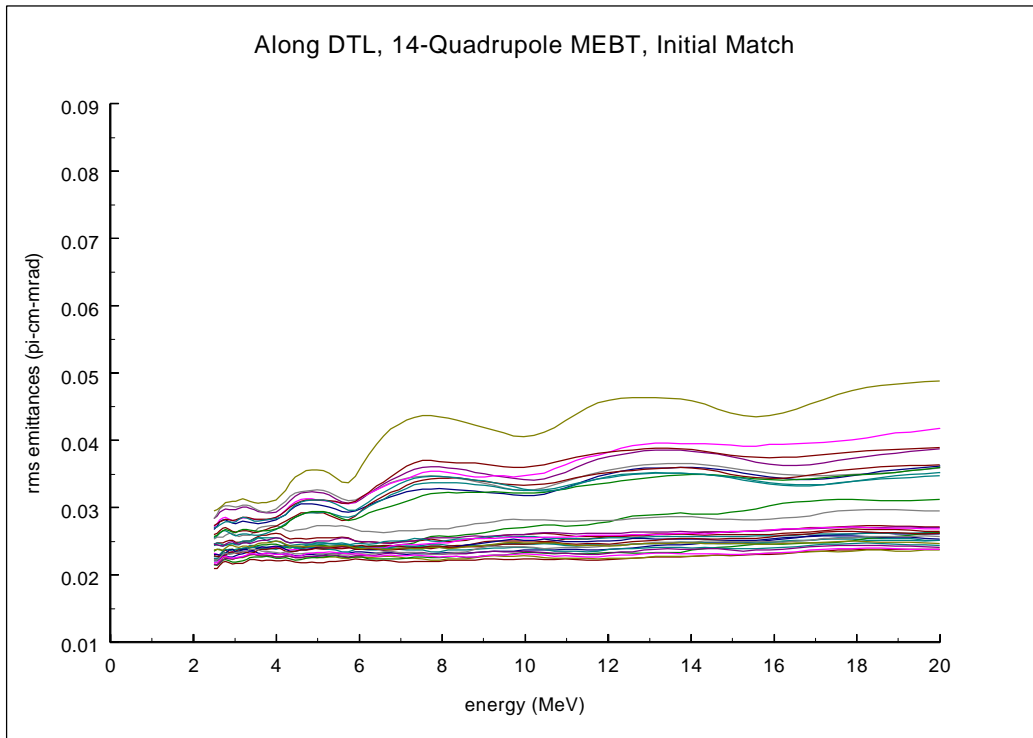


Figure 4. Transverse and longitudinal rms emittances (top) and maximum beam extents (bottom) in DTL, for initial match.

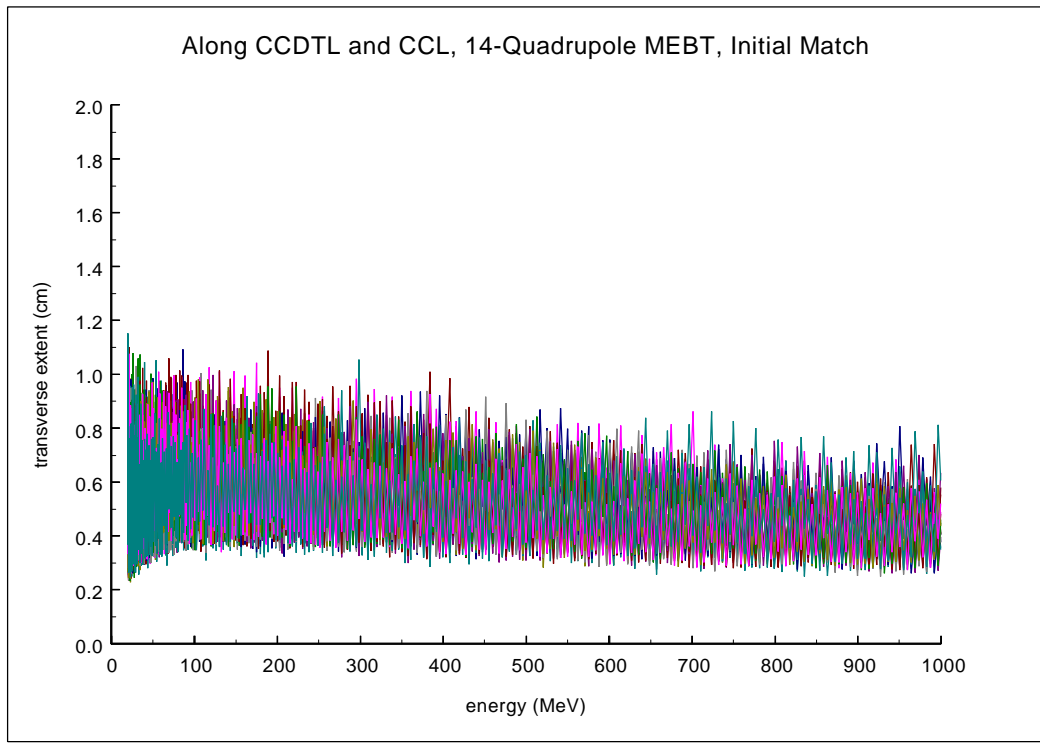
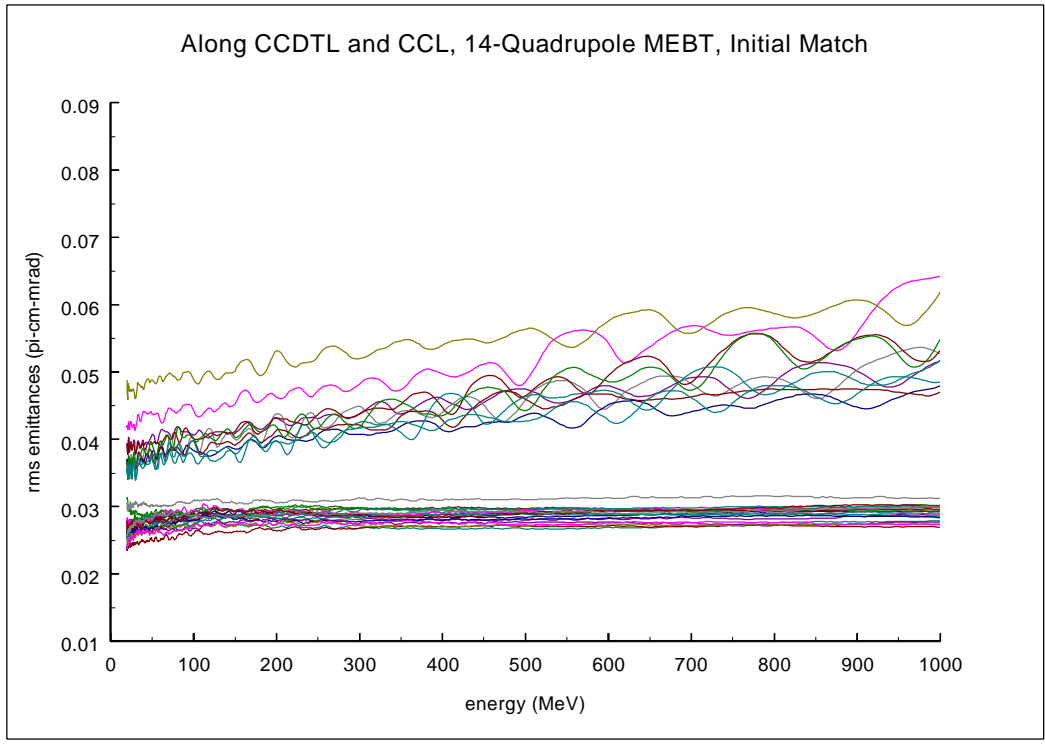


Figure 5. Transverse and longitudinal rms emittances (top) and maximum beam extents (bottom) in CCDTL and CCL, for initial match.

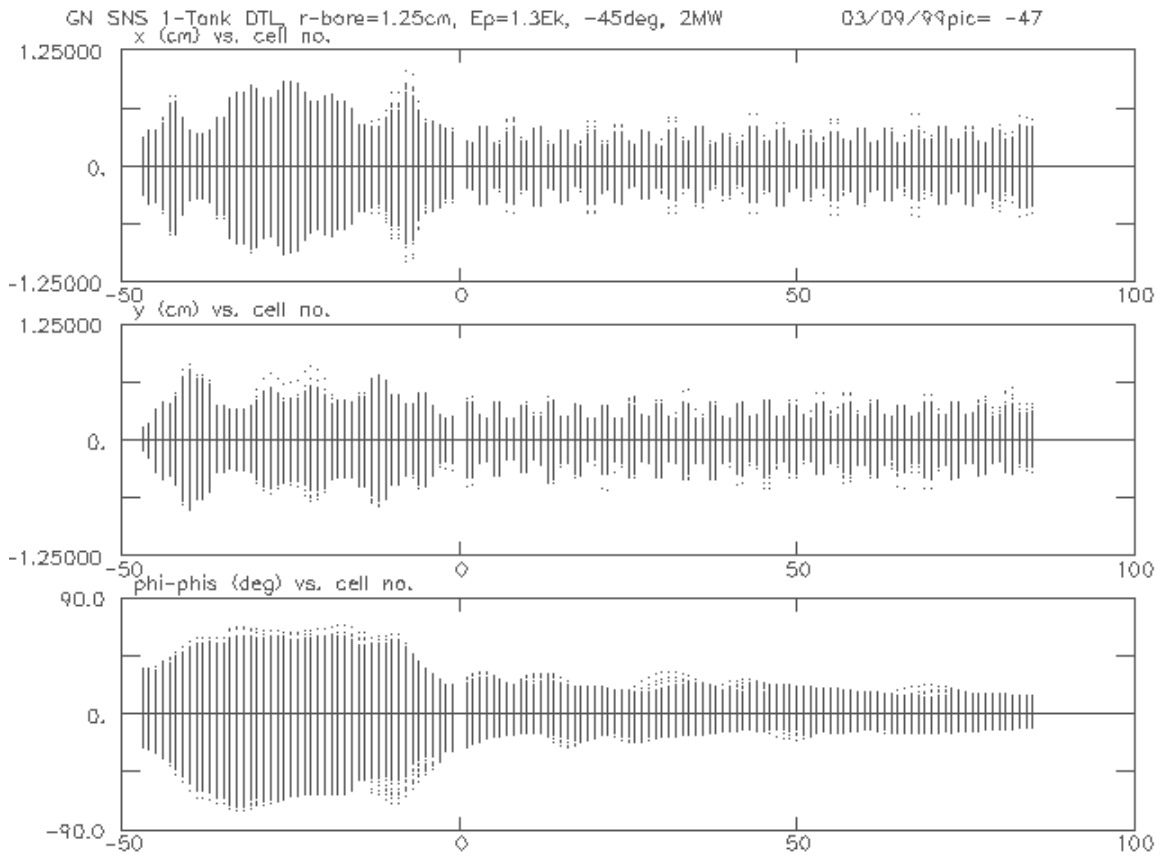


Figure 6. Beam-profile plots through MEBT and DTL,
for 14-quadrupole MEBT with improved match.

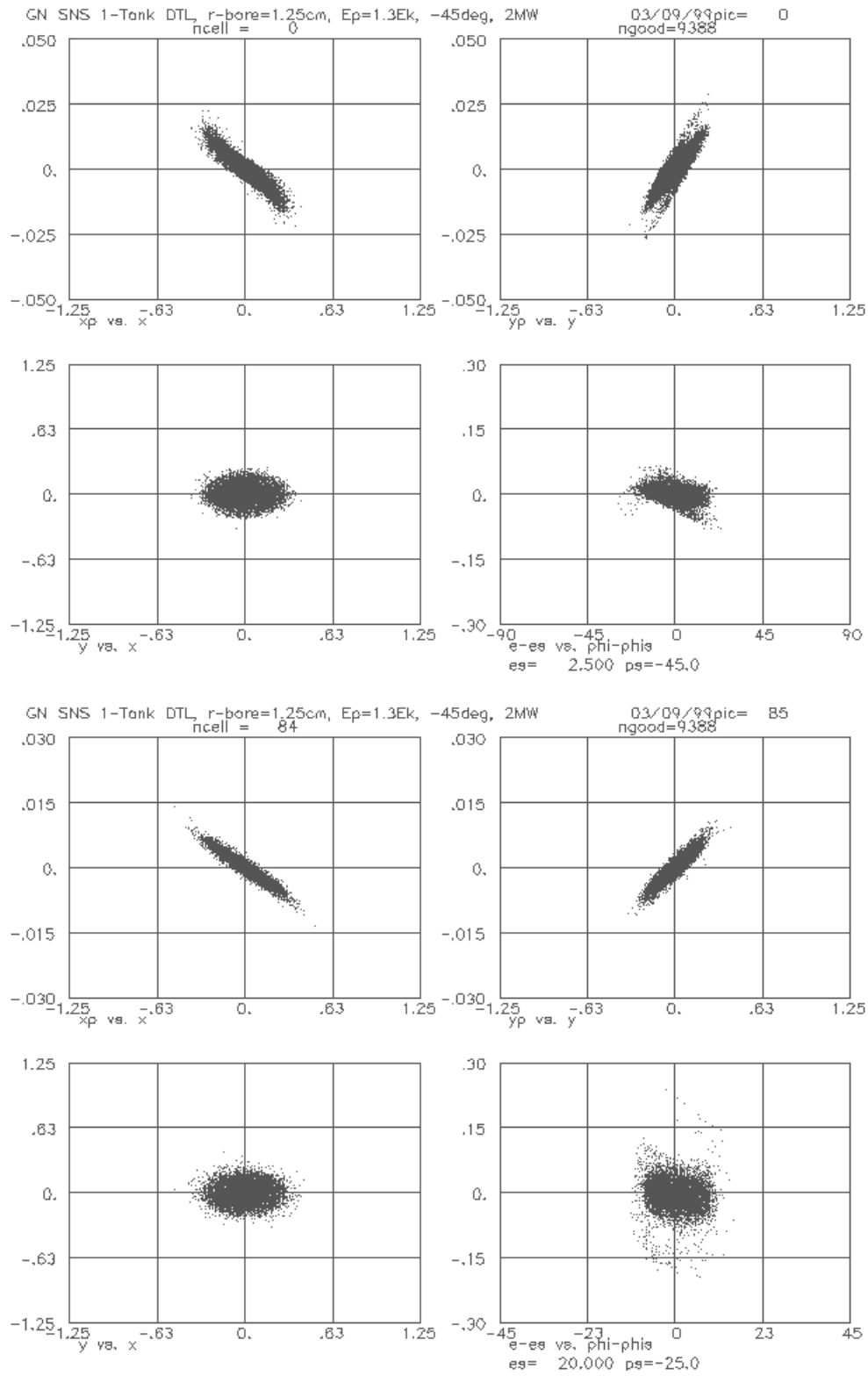


Figure 7. Beam phase-space plots at end of MEBT (top) and at end of DTL (bottom), for 14-quadrupole MEBT with improved match.

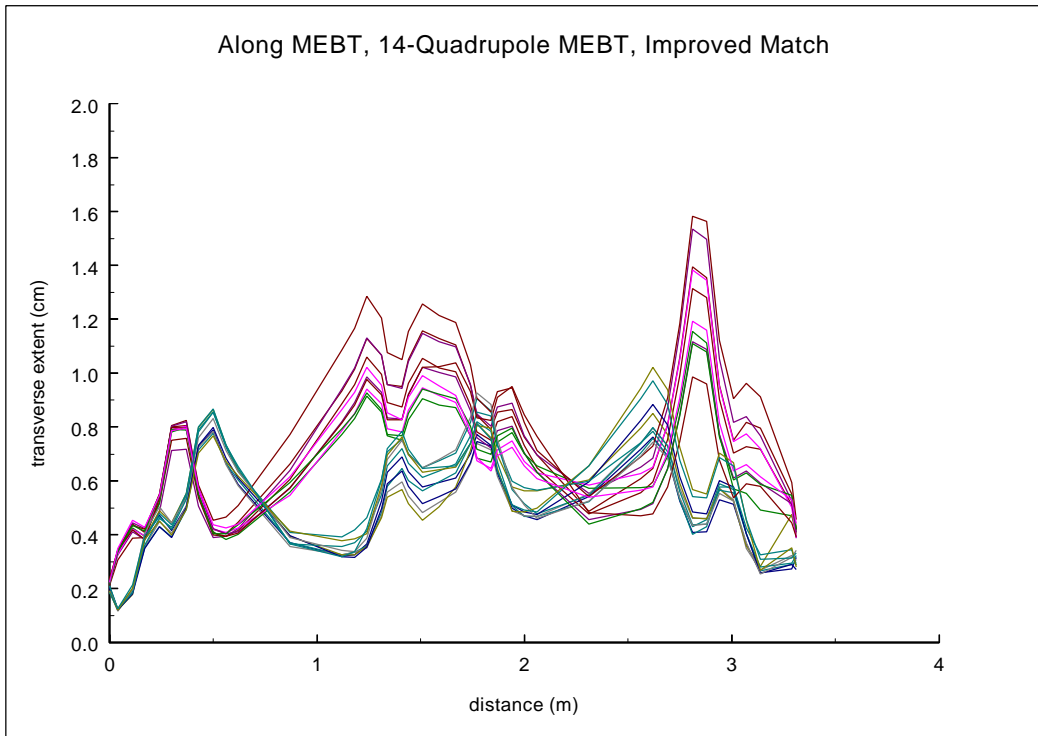
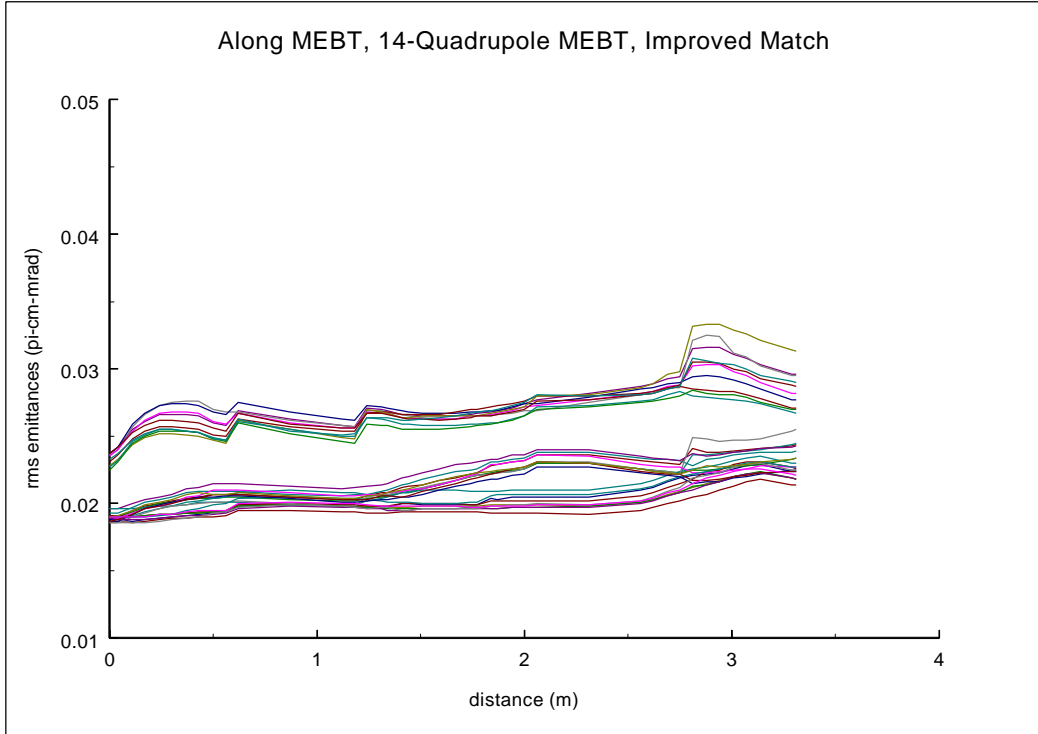


Figure 8. Transverse and longitudinal rms emittances (top) and maximum beam extents (bottom) in MEBT, for improved match.

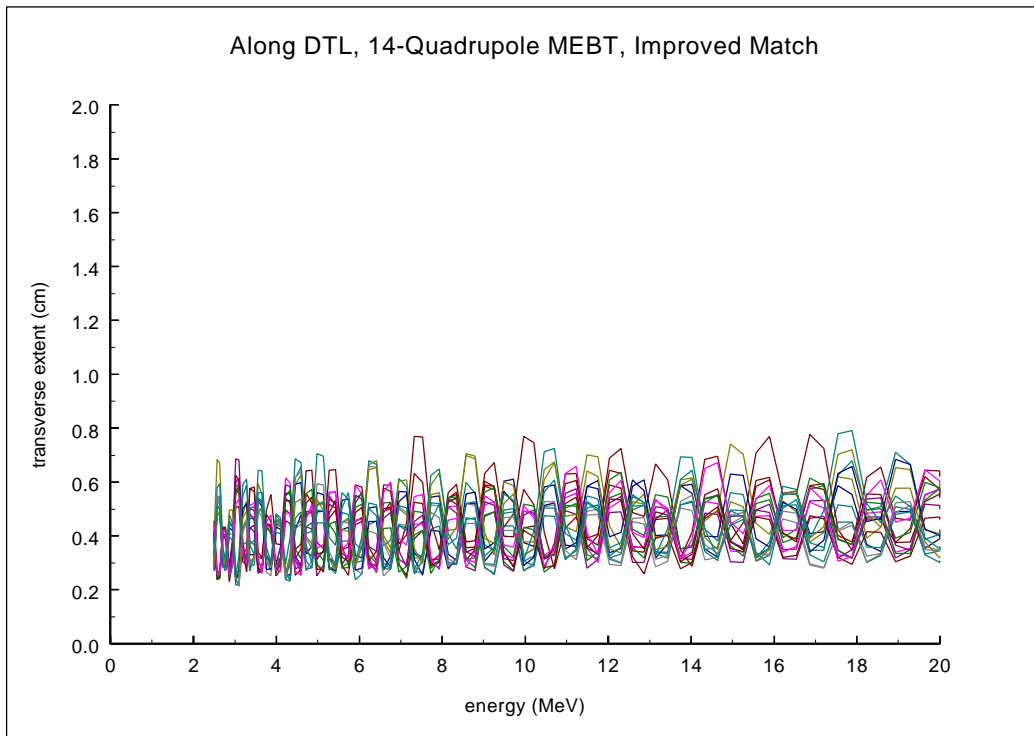
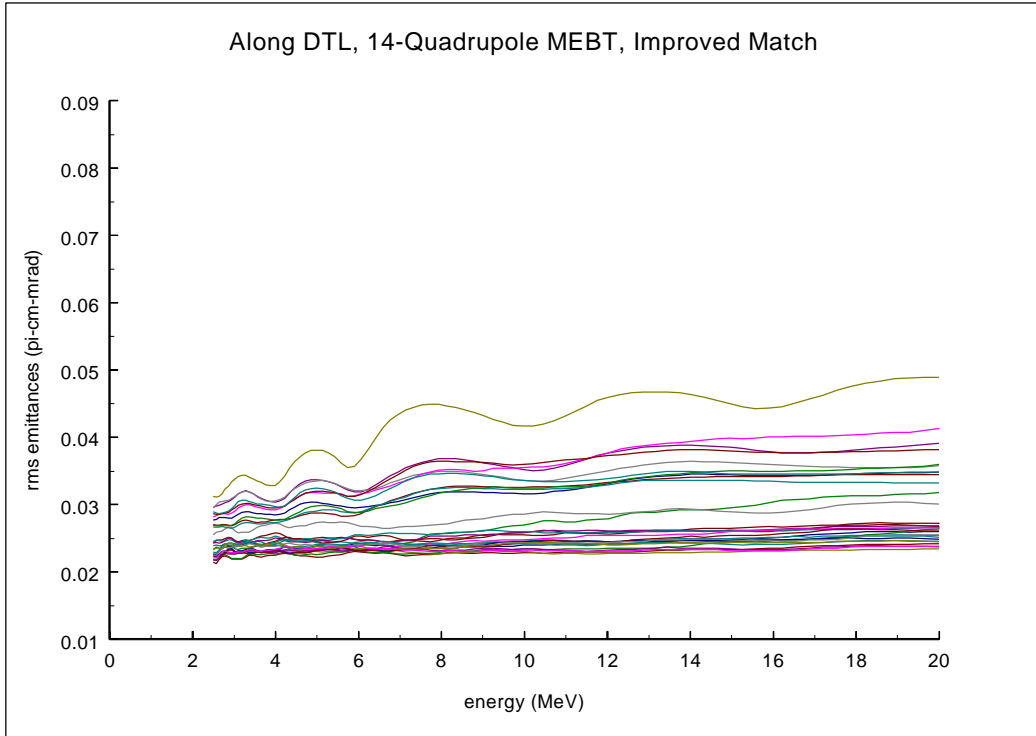


Figure 9. Transverse and longitudinal rms emittances (top) and maximum beam extents (bottom) in DTL, for improved match.

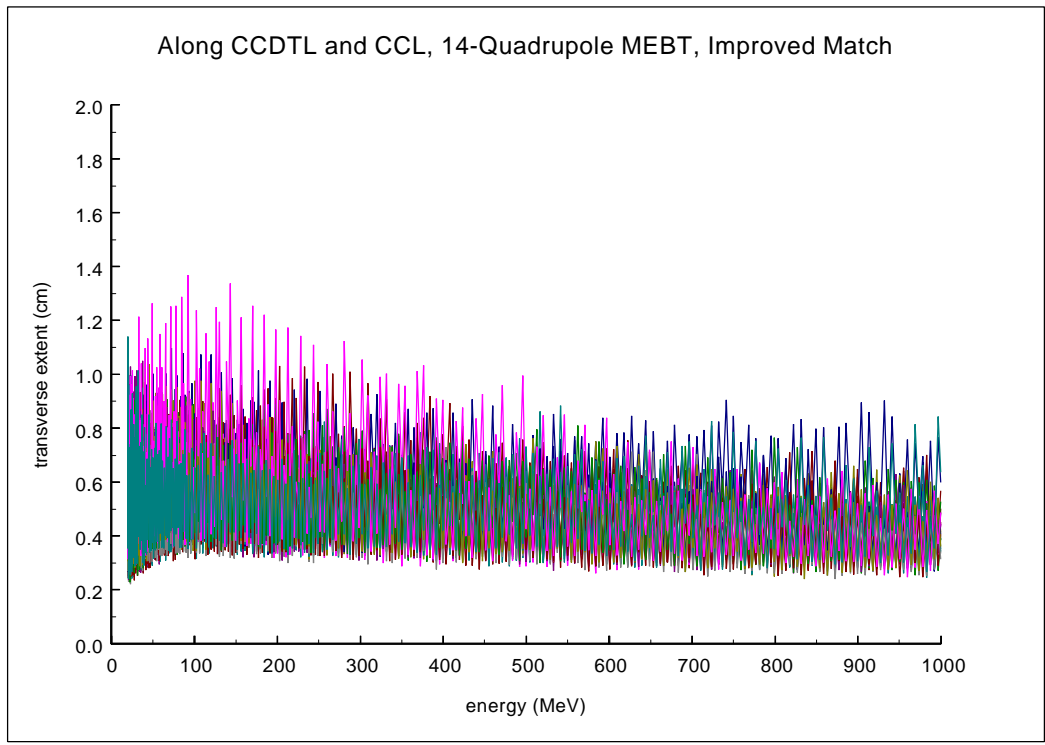
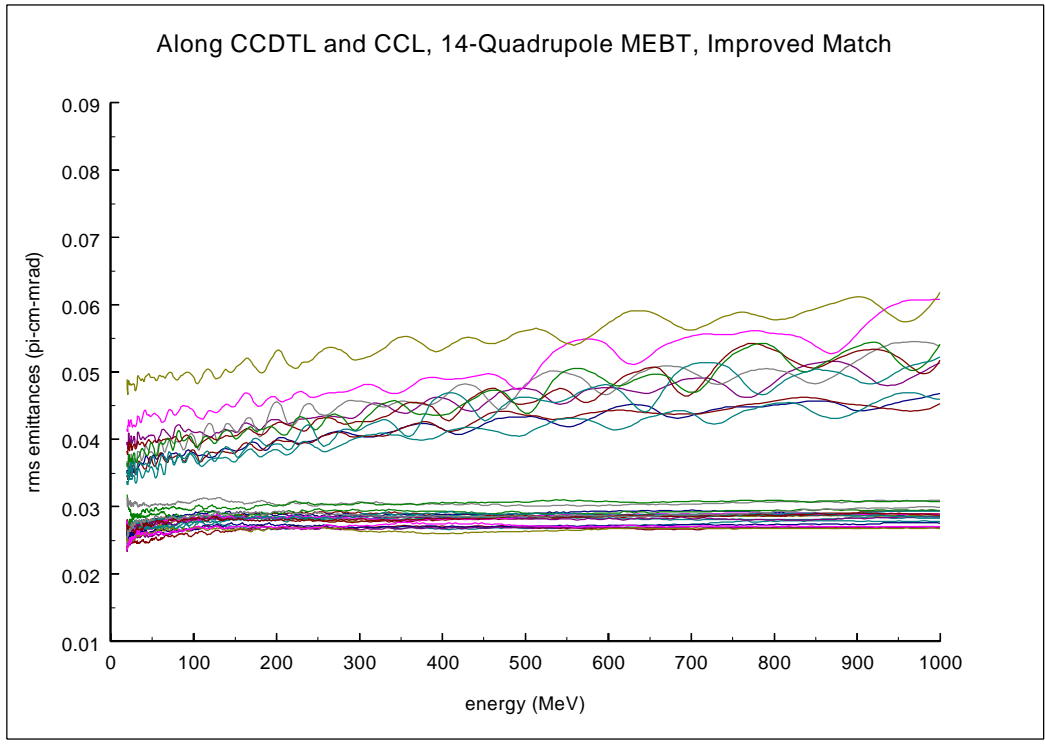


Figure 10. Transverse and longitudinal rms emittances (top) and maximum beam extents (bottom) in CCDTL and CCL, for improved match.